NASA TECHNICAL TRANSLATION

NAS TT F-13,033

A CALCULATION METHOD FOR WINGS IN STEADY OR UNSTEADY SUPERSONIC FLOW

J. M. Brun-Gabriel

Translation of "Une Méthode de Calcul des Ailes en Écoulement Supersonique Stationnaire ou Instationnaire", La Recherche Aerospatiale, No. 132, Sept. Oct. 1969, pp. 3-13.

NATIONAL AERONAUTICS AND SPACE ADMINISTRATION
WASHINGTON, D. C. 20546 MAY 1970

A CALCULATION METHOD FOR WINGS IN STEADY OR UNSTEADY SUPERSONIC FLOW

J. M. Brun-Gabriel[1, 2]

ABSTRACT. In this paper is presented a wing calculation method which, based on the source supersonic method, seeks its precision through a refined representation of the leading and the trailing edge shape, and also through the systematic study of the singularities at the leading edge. /3*

The benefit obtained from the precautions taken through a thorough study of the causes of error is outlined. A few examples of steady and unsteady flows are presented, and comparisons are made with previously used methods.

After a preliminary work done on the electric calculator, designed at the C.N.R.S. Analog Computation Center for surface integration, a program has been written for the Univac 1108 computer. This program permits a systematic exploitation thanks to the wide generality of the method and to the very short computing time involved.

Key words (NASA thesaurus): Wings — Airfoils — Leading edges — Trailing edges — Computer programming — Univac 1108 computer — Steady flow — Unsteady flow — Supersonic flow.

Notation Used /4

M : Mach number at infinity upstream

$\beta = \sqrt{M^2 - 1}$

$\vec{V}$: velocity vector

---

* Numbers in the margins indicate pagination in the original foreign text.

(1) Centre de Calcul Analogique de Centre National de la Recherche Scientifique (Center for Analog Computation, National Center for Scientific Research), 29, avenue de la Division Leclerc, 92-Chatillon.

(2) This article is the subject of a thesis for the Ph.D. examination which will be defended soon.

U : velocity modulus at infinity upstream.

U_u, U_v, U_w : perturbation velocity along the x, y, z axes.

a : speed of sound in unperturbed flow.

t : time.

ϕ : perturbation velocity potential.

ξ, η : coordinates of a current point.

X, Y, Z : coordinates after Prandtl-Glauert transformation.

λ, μ : characteristic coordinates.

ε : length of the side of a square in the axes, and of the diagonal in the x, y axes.

k_{pq}, l_{pq} : real and imaginary influence coefficients.

K_j^{pq}, K_j^i : truncation coefficients within the wing.

A_j^{pq}, A_j^i : truncation coefficients on the current sheet upstream.

K, A, B : coefficients of the development of w on the current sheet upstream.

$C_p = \frac{2(p - p_\infty)}{\rho_\infty U^2}$: pressure coefficient, p = pressure, ρ = density.

$C_x = \frac{2}{S}\iint_{wing} w.Cp\ dx\ dy$: drag coefficient.

$C_z = \frac{2}{S}\iint_{wing} Cp\ dx\ dy$: lift coefficient.

$C_{mx} = \frac{2}{SC}\iint_{wing} x.Cp\ dx\ dy$: moment coefficient.

S : wing surface.

C : center chord.

ω : vibrational frequency.

$\Omega = \frac{\omega C}{2U}$: reduced frequency.

$f_c = \frac{\Omega}{n}$: characteristic frequency.

$n \times n$: number of squares in the division.

$\delta C_z = C_z$ (calculated) $- C_z$ (analytic).

$\delta C_{mx} = C_{mx}$ (calculated) $- C_{mx}$ (analytic).

$R(\ )$: real part of.

$I(\ )$: imaginary part of.

Abbreviations Used

T. P. : thickness problem.
L. P. : lift problem.
L. E. : leading edge.
T. E. : trailing edge.
T. S. : truncated square.

I. Introduction

The source method has been proposed by Puckett [1] for calculating the thickness effect in steady supersonic flow. This method is easily applied to the lift effect when the leading edge is supersonic; difficulties appear in this application when the leading edge becomes subsonic whether or not the flow be stationary. For steady flow, Evvard [2] has proposed the well-known method of reflections, while Hancock [3] prefers inverting an integral equation; these two methods have a limited range of application. For unsteady flows, Garrick and Rubinow [4] showed the possibility of using distributions of impulse sources, which Pines and Dugundji [5] integrated numerically by the "box" method. Ta Li [6] proposed boxes whose diagonals are Mach lines, while Zartarian [7] preferred to use (along with Evvard) characteristic coordinates which determine a lattice parallel to the Mach lines. More recently, Stark [8] used a method similar to that of Zartarian by insisting on infinities in the current sheet upstream, whereas Fenain [9] inverted the integral formula after making it discrete.

In all these methods of calculation, which have led to numericalization, an accuracy of about 5% can be achieved. Improvement in the accuracy cannot be expected by increasing the fineness of the division, since computation time increases much faster than accuracy; a systematic study of causes of error and of appropriate corrections was therefore launched at the C.C.A. of the C.N.R.S. in 1961.

The solution, fairly rapidly developed for steady flows [10], was sufficiently promising that construction of an electric computer adapted to unsteady

problems was decided upon. It is due to this computer that the method described here was determined; when these results were presented to Mr. Dat, he encouraged me to transpose this method for use in a large computer. This transposition was recently accomplished for the Univac 1108, which allows systematic exploitation of the method.

II. Formulation of the Problem

Consider a flow for which the Mach number at infinity upstream is $M > 1$. Because of the assumption that perturbations are small, it is possible to linearize the equations and the boundary conditions. It is on the plane $z = 0$, called the wing plane, that the boundary conditions will be written (Figure 1). In terms of the factor U, the velocity modulus at infinity, the velocity at any point is written:

$$\vec{V} = U((1 + u)\vec{i} + v\vec{j} + w\vec{k})$$

u, v, and w are derived from the velocity perturbation potential ϕ which satisfies

$$\beta^2\varphi_{xx} - \varphi_{yy} - \varphi_{zz} = -\left(\frac{1}{a^2}\varphi_{tt} + 2\frac{M^2}{U}\varphi_{xt}\right) \tag{1}$$

with

$$\beta^2 = M^2 - 1.$$

The second term of this equation is zero when the flow does not depend on the time t.

The source method gives an integral solution of (1) in the form

$$\varphi(x, y, o^+, t) = -\frac{1}{2\pi}\iint_H \frac{w(\xi, \eta, o^+, t - \tau_1) + w(\xi, \eta, o^+, t - \tau_2)}{\sqrt{(x - \xi)^2 - \beta^2(y - \eta)^2}}\, d\xi d\eta. \tag{2}$$

The number 0^+ indicates that the solution is calculated on the wing in the upper half-space; it is convenient to consider the lower half-space by separating the thickness problem (T. P.), for which ϕ is even in z ($\phi^+ = \phi^-$), and the lift problem (L. P.), for which ϕ is odd in z ($\phi^+ = -\phi^-$).

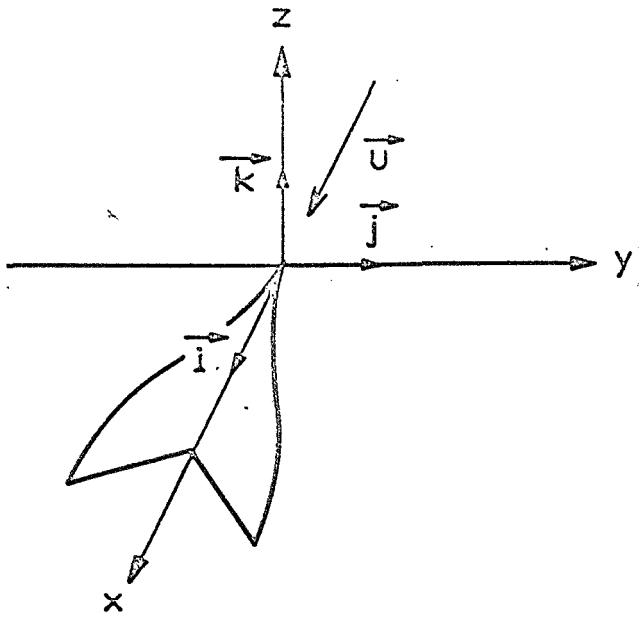

Figure 1.

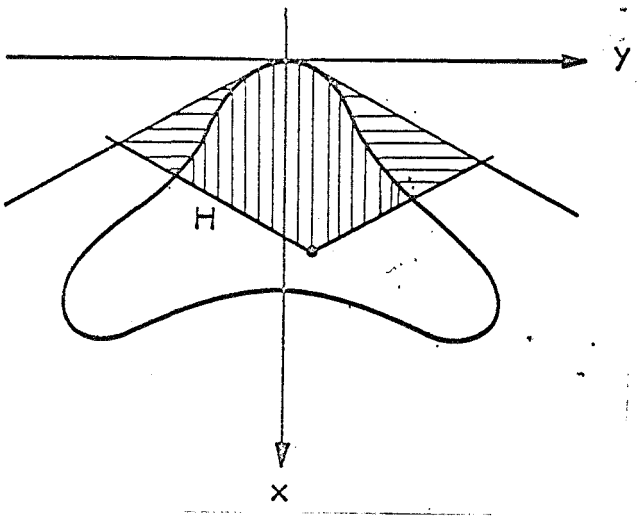

Figure 2.

The quantities τ_1 and τ_2 can be expressed as functions of the space variables:

$$\begin{cases} \tau_1 = (M(x-\xi) + \sqrt{(x-\xi^2) - \beta^2(y-\eta)^2})/a\beta^2 \\ \tau_2 = (M(x-\xi) - \sqrt{(x-\xi)^2 - \beta^2(y-\eta)^2})/a\beta^2. \end{cases} \quad (3)$$

It should be noted that in the steady-state, the waves emitted at $(t - \tau_1)$ and $(t - \tau_2)$ are identical, which makes them indistinguishable, and solution (2) is written

$$\varphi(x, y, o^+) = -\frac{1}{\pi} \iint_H \frac{w(\xi, \eta, o^+)}{\sqrt{(x-\xi)^2 - \beta^2(y-\eta)^2}} d\xi d\eta. \quad (4)$$

Whether the problem be steady or unsteady, the domain of integration H is /5 defined as the portion of the plane z = 0 which is simultaneously in the front Mach cone of point (x, y) and perturbed by the wing (Figure 2). The horizontally hatched zones can be ignored for the T. P. since the parity of ϕ makes w = 0 outside the wing. In contrast, for the L. P. ϕ is odd, and so is zero on these surfaces. Then an inverse problem must be solved to determine w.

For clarity of exposition, steady flows will be treated first, then unsteady flows in the balance of the paper.

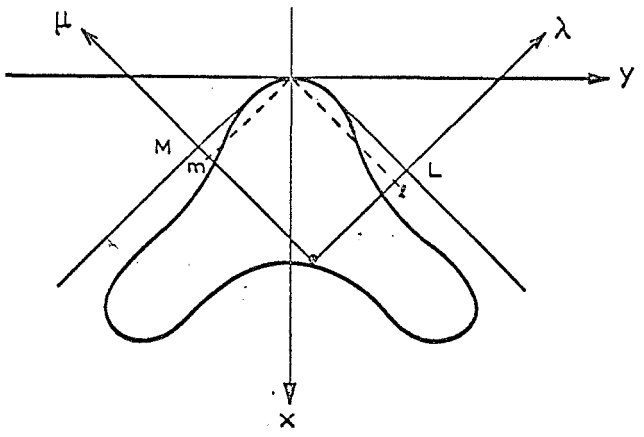

Figure 3.

III. Steady Flows

III.1. Definition of Coordinate Axes

To deal with orthogonal Mach lines, a Prandtl-Glauert transformation can be performed:

$$X = x, \quad Y = \beta y, \quad Z = \beta z. \tag{5}$$

Solution (4) is then written

$$\varphi(X_0, Y_0) = -\frac{1}{\beta\pi}\iint_H \frac{w(X, Y)}{\sqrt{(X - X_0)^2 - (Y - Y_0)^2}}\, dX dY.$$

On choosing characteristic axes centered on X_0, Y_0, this expression is simplified and the limits of integration are conveniently expressed:

$$\begin{cases} \lambda = (Y - Y_0) - (X - X_0) \equiv Y - X + l \\ \mu = -(Y - Y_0) - (X - X_0) \equiv -Y - X + m \end{cases} \tag{6}$$

$$\varphi(X_0, Y_0) \equiv \varphi(l, m) = -\frac{1}{2\beta\pi}\int_0^L \int_0^M \frac{w(\lambda, \mu)}{\sqrt{\lambda\mu}}\, d\lambda d\mu. \tag{7}$$

The quantities l and m are the coordinates of the former origin in the new axes, while L and M are the terminal limits of the perturbed domain (Figure 3).

III.2. Placing the Lattice

The division chosen for calculation of the integral is quite naturally parallel to the new λ, μ axes and thus to the Mach lines. It is desirable to define two lattices: the first, fixed to the wing, carries the boundary conditions in discrete form; the second constitutes the region of integration, which contains the influence coefficients. The integral solution is calculated at each node of the wing lattice using a form approximated by finite summation:

$$\varphi(l, m) = -\frac{2\varepsilon}{\beta\pi}\sum_{p,q=0}^{P,Q} w_{pq} k_{pq} \tag{8}$$

where

$$w_{pq} = w\left(\left(p+\tfrac{1}{2}\right)\varepsilon,\ \left(q+\tfrac{1}{2}\right)\varepsilon\right) \tag{9}$$

and

$$k_{pq} = \frac{1}{4\varepsilon}\int_{p\varepsilon}^{(p+1)\varepsilon}\frac{d\lambda}{\sqrt{\lambda}}\int_{q\varepsilon}^{(q+1)\varepsilon}\frac{d\mu}{\sqrt{\mu}} = \left(\sqrt{p+1}-\sqrt{p}\right)\left(\sqrt{q+1}-\sqrt{q}\right). \tag{10}$$

In the program for numerical computation it is anticipated that the analytic expression of the L.E. and the T.E. can vary from the root to the tip. In practice it is sufficient to specify the number and positions of the junction points and the parameters which define arcs of second-degree curves for the L.E., and of straight segments for the T.E. Such a definition of the T.E. seems sufficient since it is generally provided with flaps, which leads the manufacturers to generate it by straight segments. Further, if the study of a particular case would propose a curved T.E., absence of a singularity in the current sheet downstream would allow approximation with good accuracy without having to use too many segments.

After the program has read the set of Mach numbers for which the calculation is to be made, it takes them one by one, carries out the Prandtl-Glauert transformation, and determines the characteristic square circumscribing the wing (Figure 4). The wing lattice is then constructed as a function of the fineness of the desired division.

By considering the symmetry or antisymmetry in Y, one can generally limit the calculation to those points of the wing where $Y \geq 0$, which moreover leads to a determination of the precise limits for the calculation of ϕ or of the influence coefficients k_{pq}. All these precautions avoid calculation of ϕ at useless points, and where the number of squares appearing in the finite sum is greatest. The limit to the calculation of the k_{pq} is especially important for unsteady problems where the table of the k_{pq} is really a double index, and represents a substantial part of the computing time.

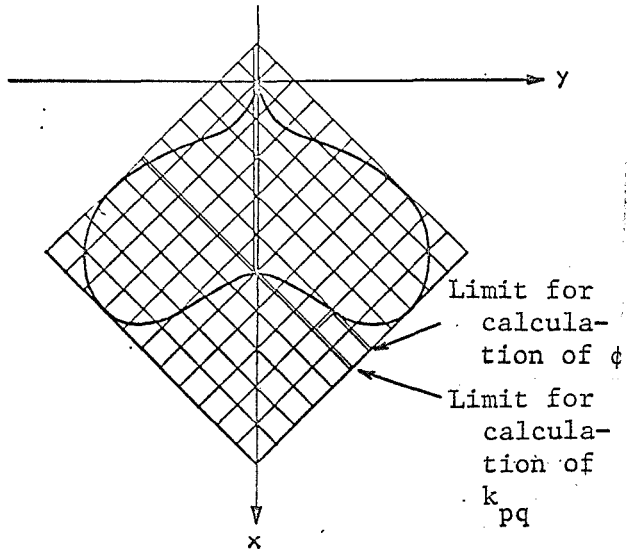

Figure 4.

III.3. Lack of Precision Due to Discrete Integration

Discrete integration gives an exact result only if the function to be integrated is effectively constant on each element of area. Since the singularities in the kernel are included in the computation of the influence coefficients k_{pq}, it is only the variations of $w(\lambda, \mu)$ which can lead to lack of accuracy.

In practice, the lack of accuracy is slight if $w(\lambda, \mu)$ is continuous, and a reasonably fine division (20 x 20) allows good accuracy (0.5%). A rather fine division is also necessary for good evaluation of the overall values. In contrast, a discontinuity in the slope leads to large errors, called truncation errors, which generally appear at the L.E. This discontinuity can be finite (for a T.P. or for an L.P. at a supersonic L.E.) or infinite (for an L.P. along a subsonic L.E.). This last case is the more ticklish to treat, since the infinite slopes are to be determined by solving an inverse problem: as has been shown in Section II, the condition to be imposed outside the wing is $\phi = 0$.

Most computational methods have sought to avoid the necessity of point-by-point inversion outside the wing. The most general and most elegant of these was proposed by M. Fenain and D. Guiraud-Vallée [9]. By considering that all the squares are completely filled, and that the slope is constant on each square, they could invert the linear transformation which gives ϕ as a function of w. Having thus computed the inverse influence coefficients, they could express $\phi(P)$ on the wing as a function of the slope of the square whose downstream extension is at P, and of previously computed values of ϕ upstream from P. This avoids computing slopes outside the wing, and saves computer time, especially if the Mach number is small. However, to obtain very accurate results would require much too fine a division: it would overload the memory and require too much computer time.

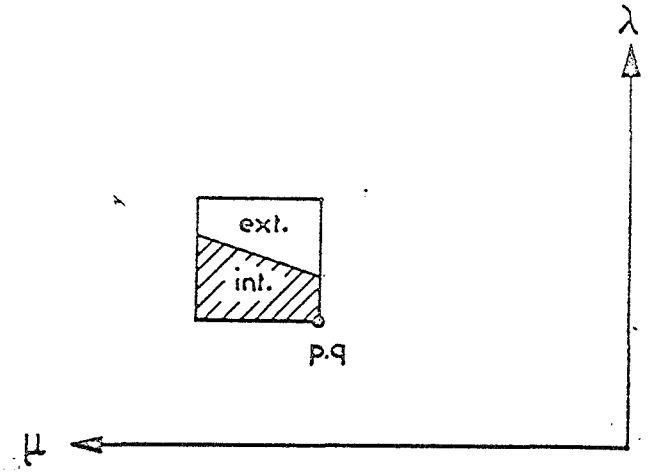

Figure 5.

For such a more subtle analysis it is necessary to consider the exact form of the L.E. (not to consider that all the squares are completely filled); it is also necessary not to neglect the form of the local infinities (not to suppose that the slope is constant over each square).

III.4. Influence of That Portion of a Truncated Square Which Is Inside the Wing

This is the only part which has any influence in the T.P., or when the L.E. is supersonic, because w = 0 outside the wing.

It can be considered that the slope is constant on the wing and that the L.E. is a straight line within any one truncated square (T.S.). A T.S. is thus subdivided into two trapezoids (Figure 5).

It is then easy to calculate the truncation coefficients K_j^{pq}, where the index j relates to the form of the T.S. under consideration, and pq its place in the region of integration.

$$K_j^{pq} = \frac{\iint_{\text{int.}} \frac{d\lambda d\mu}{\sqrt{\lambda\mu}}}{4\varepsilon k pq}. \tag{11}$$

This computation could be carried out for each square j and each position pq, i.e., for each point of the calculation.

This solution would be incontestably accurate, but it would considerably increase the computation time.

If the coefficients K_j^{pq} are not equal to the cross-hatched areas of the wing in Figure 5, it is principally because of singularities in the kernel $\frac{1}{\sqrt{\lambda\mu}}$. These singularities lie on the lines $\lambda = 0$ and $\mu = 0$, so it is logical to make sure that the variation of K_j^{pq} is small for all computational points where, for example, $p = 0$ and $q \neq 0$. Depending on the form of the T.S. considered, the difference δK_j^a between K_j^{01} and K_j^{0q} is variable; but if this difference increases with q, it is weighted with the influence coefficient K_{0q} which decreases when q increases. Finally, $k_{0q}\delta K_j^q \sim 0.001$, to be compared to the influence coefficient $k_{00} = 1$. /7

Because of this fact, it is sufficient to compute four constants for each T.S. once and for all at the beginning of the computation.

$K_j^1 \equiv K_j^{00}$ corresponds to $\lambda = 0, \mu = 0$
$K_j^2 \equiv K_j^{01} \simeq K_j^{0q}$ corresponds to $\lambda = 0, \mu \neq 0$
$K_j^3 \equiv K_j^{10} \simeq K_j^{p0}$ corresponds to $\lambda \neq 0, \mu = 0$
$K_j^4 \equiv S_{int} \simeq K_j^{pq}$ corresponds to $\lambda \neq 0, \mu \neq 0$.

The coefficient $K_j^4 \equiv S_{int}$ is the proportionality constant at the interior surface of the square.

Depending on the values of p and q (i.e., the point of computation), one of these four constants K_j^i is chosen.

III.5. Influence of Infinite Discontinuities

Two cases can be presented: L.E. curved, or L.E. subsonic in an L.P.

In the case of a curved L.E., there is a direct problem, since the curve is known; this effect can be computed separately, which adds a contour integral (not treated here). The suction effect of a curved subsonic L.E. will not be considered further.

For a subsonic L.E. in the L.P., the problem is mixed, and the infinity of the current surface cannot be treated separately — it is included in the

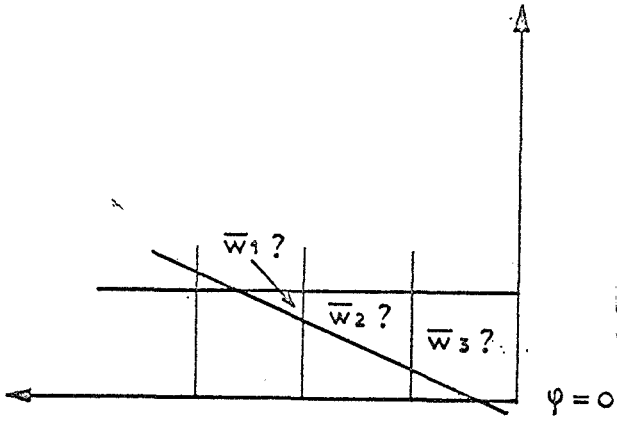

Figure 6.

solution of the inverse problem which allows the condition $\phi = 0$ to be satisfied outside the wing.

Further, the L.E. determines the truncation of many squares before the condition $\phi = 0$ can be written. The problem is thus indeterminate (Figure 6).

By neglecting the curvature of the current surface it is possible to assume that there is a constant average slope on the portion of the T.S. outside the wing. The indeterminacy is then removed by the further supposition that this average slope does not vary from one square to another.

Such a procedure correctly represents the L.E. thanks to the coefficients K_j^i and $(1 - K_j^i)$ which affect the parts interior and exterior to the wing, respectively. However, the overall results are mediocre, as can be anticipated from the oscillation of the values of C_p, which can be as much as 50%. This oscillation is two or three times smaller than if the form of the T.S. is not considered, and it expresses the influence of the curvature of the current sheet near the L.E.

The truncation coefficients "upstream" must then include not only the form of the truncation, but also the curvature of the current sheet:

$$\overline{\overline{A^{pq}_{ij}}} = \frac{\iint_{\text{ext}} \frac{w(\lambda, \mu)}{\sqrt{\lambda\mu}}\, d\lambda d\mu}{4\varepsilon k_{pq}}. \qquad (12)$$

Because of the predominant influence of the singularity lines, four coefficients A_j^i are enough. They are defined by the same process as the K_j^i.

Study of conical flow [11] provides knowledge of the form of this current sheet. Carrying out a limited development, one finds:

$$w = w_0 \left[1 + \frac{K}{\sqrt{d}} \left(1 + Ad + Bd^2 + O(d^3) \right) \right] \qquad (13)$$

where w_0 is the angle of attack of the wing, and d is the distance between the L.E. and the point of the current sheet where w is computed, measured along a characteristic line (d = 0 at the L.E. and d = 1 at the apex). Such a development can be carried out for any wing. The coefficient K includes the local sweep of the wing, which determines the "intensity" of the infinity; it is thus the same as that for a conical wing of the same sweep angle. The coefficient B is modified to include terms of $O(d^3)$, and brings about the fit w = 0 at the apex by writing $B = -(\frac{1}{K} + A + 1)$. The coefficient A acts on the curvature at a certain distance from the L.E. It is influenced by the shape of the portion of the wing which is intercepted by the forward Mach cone of the point on the leading edge, as well as by the distribution of slopes within this portion of the wing. It is impossible in practice to include all these parameters, but even a large variation of A will automatically be compensated by the simultaneous variation of B, and is expressed only by very small differences in the proportionality relationships among the upstream truncation coefficients A^i_j. /8

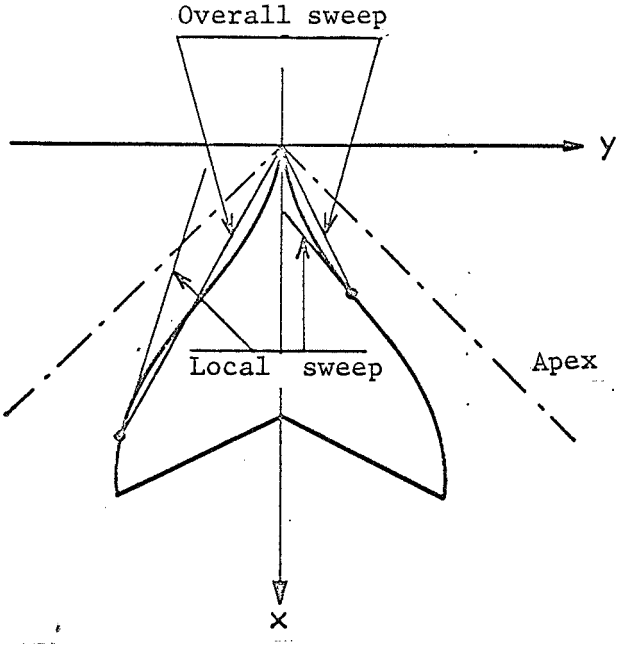

Figure 7.

Indeed, only these proportionality relations have any influence, since the general amplitude of the upstream slopes is controlled by the condition $\phi = 0$. This is why the choice of the coefficient A corresponding to a conical wing with sweep equal to the mean between the local and the general sweep angles (Figure 7) is a satisfactory approximation. This is, of course, a better approximation than that of using only the term A and making it fit w = 0 at the apex.

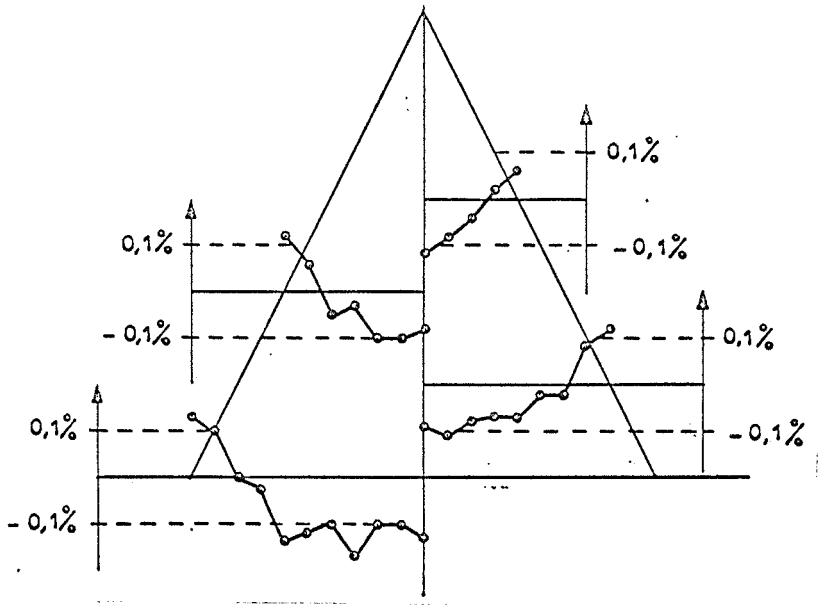

Figure 8.

The oscillation of C_p is reduced to less than 5% even if the flow is not conical, which shows a posteriori the good basis of the discussion above.

III.6. Precision Obtained

The group of corrections presented in III.4. and III.5. give the velocity potential with an accuracy of the order of 0.2% for the thickness effect, and 0.5% for the lift effect (relative errors of the local values with respect to the maximum value of ϕ). Figure 8 gives the distribution of these errors for various sections x = constant for a delta wing with lozenge profile (T.P.).

To compute the overall values it is necessary again to differentiate to obtain C_p', and to integrate the product $f(x, y) \cdot C_p$ over the entire wing. Depending on whether C_x, C_{mx}, or C_z is to be computed, one takes

$$f(x, y) = w(x, y),\ f(x, y) = x \text{ or } f(x, y) = 1.$$

In unsteady flow, f(x, y) will be the displacement of the associated mode for the computation of the generalized forces. In that case it is important not to lose the accuracy obtained in the computation of ϕ. Errors can be introduced

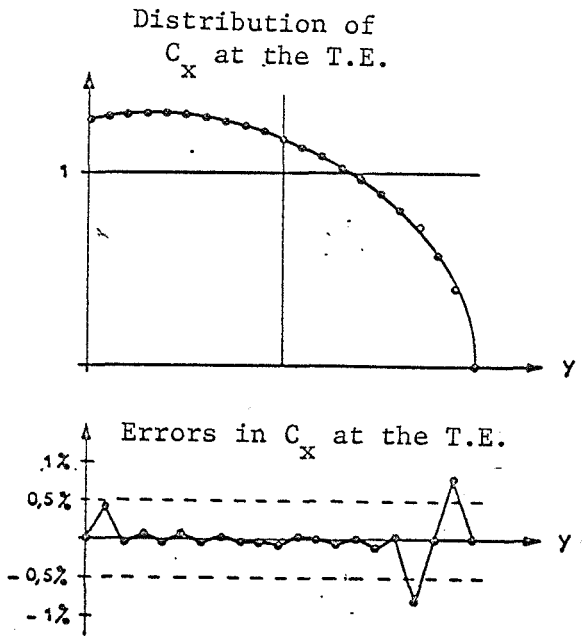

Figure 9.

from the necessity of interpolating ϕ at the L.E. and at the T.E. A linear interpolation can be insufficient at the L.E., the most delicate case being that where the L.E. and T.E. are in consecutive squares, or even in the same square. This often occurs at the wing tip, which is also a region of high gradient of the overall values. The final error can thus become greater than 1% if certain precautions concerning the curvature of ϕ are not taken (they will not be discussed here). Figure 9 shows, however, the distribution curve of C_x at the T.E. and the error in that distribution for the wing shown in Figure 8. After integration of curve 9, one finds $C_x = 2.1086$ (analytic value is $C_x = 2.10757$); the error in the overall value is thus 0.05%, which is explained by a certain compensation of errors in ϕ during the final integrations.

As Zartarian has proposed [7], it is possible to compute the overall values directly, without going through C_p. In fact, the difficulties are the same, and identical precautions yield an equivalent result. Thus it should be considered that computation of C_p is a supplementary step whose sole purpose is the localization and evaluation of the errors committed. The corresponding computer time is very short in the overall scheme, which justifies use of this intermediate step.

IV. Unstable Flows /9

Thanks to harmonic analysis the slope can be written

$$w(x, y, o^+, t) = \sum_{m=1}^{M} \sum_{l=1}^{L} e^{i\omega_l t} w_m (x, y, o^+). \qquad (14)$$

The linearity of the equations permits study of each case separately, and final summation of the results. It is fundamental that the multiplicity of cases to be studied requires very rapid solution of each one; the solutions to be adopted must not be too burdensome on machine time.

Consider a movement of frequency ω; the displacement is written

$$w(x, y, o^+, t) = e^{i\omega t}\, w(x, y, o^+). \tag{15}$$

After transformations identical to those of the steady case, solution (2) can be written as

$$\varphi(x, y, o^+, t) = -\frac{e^{i\omega t}}{2\pi\beta}\int_0^L\int_0^M \frac{w(\lambda, \mu)e^{-iK(\lambda+\mu)}\cos(J\sqrt{\lambda\mu})}{\sqrt{\lambda\mu}}\,d\lambda d\mu. \tag{16}$$

Inserting relations (3) into Formula (2) yields

$$K = \frac{\omega M}{2a\beta^2} \quad \text{and} \quad J = \frac{\omega}{a\beta^2}.$$

It is easy to construct a lattice identical to that proposed for the steady case, and so it is possible to compute ϕ by a finite summation:

$$\frac{2\pi\beta}{\varepsilon e^{i\omega t}}\,\varphi(x, y, o^+, t) \equiv \Psi(x, y) \simeq \sum_{p,q=0}^{P,Q} F_{pq}\,K_{pq} \tag{17}$$

where

$$\begin{cases} F_{pq} = w\left(\left(p+\frac{1}{2}\right)\varepsilon,\ \left(q+\frac{1}{2}\right)\varepsilon\right) = f_{pq} + i\,g_{pq} \\ K_{pq} = k_{pq} - i\,l_{pq} \end{cases} \tag{18}$$

with

$$k_{pq} = \frac{1}{4\varepsilon}\int_{p\varepsilon}^{(p+1)\varepsilon}\int_{q\varepsilon}^{(q+1)\varepsilon} \frac{\cos\left(K(\lambda+\mu)\right)\cos\left(J\sqrt{\lambda\mu}\right)}{\sqrt{\lambda\mu}}\,d\lambda d\mu \tag{19}$$

and

$$l_{pq} = \frac{1}{4\varepsilon}\int_{p\varepsilon}^{(p+1)\varepsilon}\int_{q\varepsilon}^{(q+1)\varepsilon} \frac{\sin\left(K(\lambda+\mu)\right)\cos\left(J\sqrt{\lambda\mu}\right)}{\sqrt{\lambda\mu}}\,d\lambda d\mu. \tag{20}$$

The real part k_{pq} of the influence coefficient K_{pq} has as its limit the steady influence coefficient when the frequency ω approaches zero: this is why the same notation is given it.

It is important to include the term $e^{-iK(\lambda + \mu)}$ in the kernel. This term varies fairly rapidly, independently of the mode F_{pq} considered, and systematically opposite to the variation of $\frac{1}{\sqrt{\lambda\mu}}$, for the 1_{pq} term, along with the singularity lines.

Computation of the unsteady influence coefficients is much more delicate than that of the steady coefficients. The accuracy of their computation affects the whole accuracy of the results, which is why special care has been given it.

IV.1. Computation of the Influence Coefficients

Computation from first principles cannot go beyond the first integral, where the expression is already in Fresnel integrals. As numerical integration is necessary, it is more effective to return the problem to its source. Retaining the basic kernel $\frac{1}{\sqrt{\lambda\mu}}$, the surfaces $\cos(K(\lambda + \mu))\cos J(\sqrt{\lambda\mu})$ and $\sin(K(\lambda + \mu))\cos(J\sqrt{\lambda\mu})$ are approximated by integrable limited developments: this has been done is Figure 10 by passing a second-degree surface through nine points of each square. When the frequency increases or the Mach number decreases, it can be necessary to subdivide into four those squares adjacent to singularity lines. With this method, computational time can be minimized by storing the values of $\cos(K(\lambda + \mu))$ and $\sin(K(\lambda + \mu))$ for the whole computation, and retaining border values common to two squares. The results are very accurate, each coefficient being computed with accuracy greater than 10^{-4}.

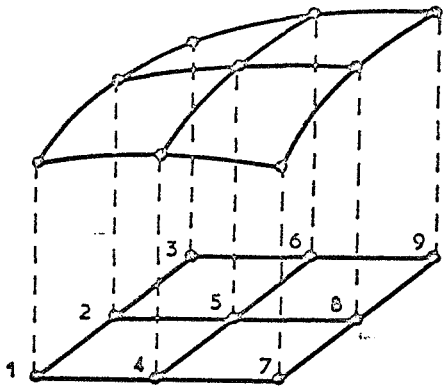

Figure 10.

IV.2. Truncation Errors

These are fundamentally the same as those of the steady case treated in III.4. and III.5. To handle the truncation effects perfectly, it would be necessary to consider the complete kernel of the integral, as is done for the influence coefficients. The complication and computer time which such a solution would

require lead to use of only the principal part of the kernel $-\frac{1}{\sqrt{\lambda\mu}}-$ and to the assumption for the calculation that the movement is quasi-stationary in each T.S. The validity of this hypothesis has been confirmed by a systematic study of a rectangular wing with finite or infinite span in bending or torsion (the only cases with analytic solutions for comparison [12, 13].

IV.3. Rectangular Wing of Infinite Span in Bending

The only errors to be considered in this calculation are:

(a) truncation "internal" to the wing,
(b) computation and integration of the C_p.

Indeed, the computation of the influence coefficients can be considered perfect in regard to causes (a) and (b). The errors of type (a) are roughly proportional to the truncation surface and they increase with the "characteristic frequency" $f_c = \Omega/n$, where n is the number of squares over the chord. This characteristic frequency can be considered to be the reduced frequency relative to one square, and no longer to the whole wing. To eliminate this factor, the study was made with $f_c = 0.1$, which corresponds to ten squares over the chord for $\Omega = 1$. The truncation surface varies from single to double when /10
Ω goes from 1 to 0.5. It is seen in Table I that the truncation errors and those due to computation of the overall values tend to compensate each other. Indeed, the error is small for the real part of C_z when Ω decreases (i.e., when the truncation surface increases), and for the imaginary part of C_z it changes sign. In the case of C_{mx} the compensation is no longer so systematic, but the error is never greater than 0.2%.

It should be recalled that reduced frequencies other than 1 are treated with a limited number of squares, and that the precision of these computations can be improved. The purpose of this study is solely to evaluate the importance of causes of error (a) and (b).

TABLE I.

M = 2. Length = ∞. Bending.

Ω	$100\mathcal{R}(\delta C_z)/\lvert C_z\rvert$	$100\,\mathcal{I}(\delta C_z)/\lvert C_z\rvert$	$100\mathcal{R}(\delta C_{mx})/\lvert C_{mx}\rvert$	$100\,\mathcal{I}(\delta C_{mx})/\lvert C_{mx}\rvert$
0,5	+ 0,15	— 0,1	— 0,13	0,15
0,6	+ 0,11	— 0,10	— 0,10	0,13
0,7	+ 0,08	— 0,09	— 0,07	0,14
0,8	+ 0,06	— 0,06	— 0,05	0,15
0,9	+ 0,05	+ 0,003	— 0,02	0,19
1	+ 0,05	+ 0,015	+ 0,01	0,18

TABLE II.

M = 2. Length = ∞. Torsion.

Ω	$100\,\mathcal{R}(\delta C_z)/\lvert C_z\rvert$	$100\,\mathcal{I}(\delta C_z)/\lvert C_z\rvert$	$100\mathcal{R}(\delta C_{mx})/\lvert C_{mx}\rvert$	$100\,\mathcal{I}(\delta C_{mx})/\lvert C_{mx}\rvert$
0,5	— 0,24	1,59	— 0,41	1,59
0,6	— 0,28	1,44	— 0,45	1,38
0,7	— 0,31	1,31	— 0,47	1,21
0,8	— 0,36	1,19	— 0,48	1,05
0,9	— 0,42	1,06	— 0,50	0,90
1	— 0,44	0,98	— 0,52	0,80

TABLE III.

M = 2. Ω = 1. Bending. Length *A* variable.

$\beta\mathcal{A}$	$100\,\mathcal{R}(\delta C_z)/\lvert C_z\rvert$	$100\,\mathcal{I}(\delta C_z)/\lvert C_z\rvert$	$100\mathcal{R}(\delta C_{mx})/\lvert C_{mx}\rvert$	$100\mathcal{I}(\delta C_{mx})/\lvert C_{mx}\rvert$
1	— 0,05	— 0,15	— 0,15	— 0,06
1,2	— 0,04	— 0,27	— 0,14	0,00
1,4	— 0,03	— 0,22	— 0,13	0,05
1,6	— 0,02	— 0,20	— 0,12	0,08
1,8	— 0,01	— 0,17	— 0,11	0,12
2	— 0,004	— 0,16	— 0,11	0,14

IV.4. Rectangular Wing of Infinite Span in Torsion

The variation of boundary conditions within a single square, cause (c), is added to those errors already studied. This type of error becomes larger as the division becomes coarser. Since the boundary conditions are

$$w_m(x, y) = 1 + i(2\Omega x)$$

the variation occurs in the imaginary part, when the preponderant influence coefficients near the singularity lines are the real coefficients k_{pq}. This means that the new cause of error must be more sensitive in the imaginary parts of C_z and C_{mx} than in their real parts. It is very characteristic to see this error increase when the division becomes coarser, i.e., when Ω approaches 0.5. With normal division the accuracy remains better than 1%, however (Table II).

IV.5. Rectangular Wing of Finite Span

On decreasing the length, there is an increase in the magnitude of the errors due to determination of the slopes of the current sheet upstream (d).

The bending study (Table III) shows that variation of length has little influence on the accuracy, and that the errors are analogous to those for bending

TABLE IV.

M = 2. Ω = 1. Torsion. Length A variable.

βA	$100\ \mathcal{R}(\delta C_z)/\lvert C_z\rvert$	$100\ \mathcal{J}(\delta C_z)/\lvert C_z\rvert$	$100\mathcal{R}(\delta C_{mx})/\lvert C_{mx}\rvert$	$100\mathcal{J}(\delta C_{mx})/\lvert C_{mx}\rvert$
1	— 0,27	1,11	— 0,60	0,77
1,2	— 0,31	1,09	— 0,62	0,75
1,4	— 0,33	1,08	— 0,63	0,74
1,6	— 0,35	1,07	— 0,63	0,73
1,8	— 0,36	1,06	— 0,63	0,72
2	— 0,37	1,04	— 0,63	0,71

of an infinite span. This result is very remarkable, for the upstream truncation correction assumes that the flow is quasi-steady, and the fact that the flow is not conical would have led one to expect a poor determination of the A term of Formula (13).

The torsion study (Table IV) confirms that the errors (d) are sufficiently small that the result will be as good as that for the wing of infinite span.

The whole study of the rectangular wing indicates that it is not useful to refine the determination of the truncations in unsteady flow, since, thanks to those used here, it is the variation of the slope within the non-truncated squares which becomes preponderant.

A finer division would allow an improvement in the accuracy, but would /11
considerably increase the computing time; therefore, a study of convergence for variable division seemed the most effective way to increase the precision. Working with (n x n), (2n x 2n) and (4n x 4n) divisions, the time for computation is 1.1 times that for the (4n x 4n) alone; the first two results allow calculations of a correction which corresponds to passing to (8n x 8n), which would require a computing time of the order of 16 times that for the (4n x 4n).

And so, thanks to the truncation corrections, the variation of results as a function of the division is a regular function, monotone for the cases studied until now, and not restricted to those presented in this paper.

To calculate the convergence correction, one sets

$$C_z = C_z(n) + \int_0^\infty \frac{dC_z}{dm}\, dm \qquad (21)$$

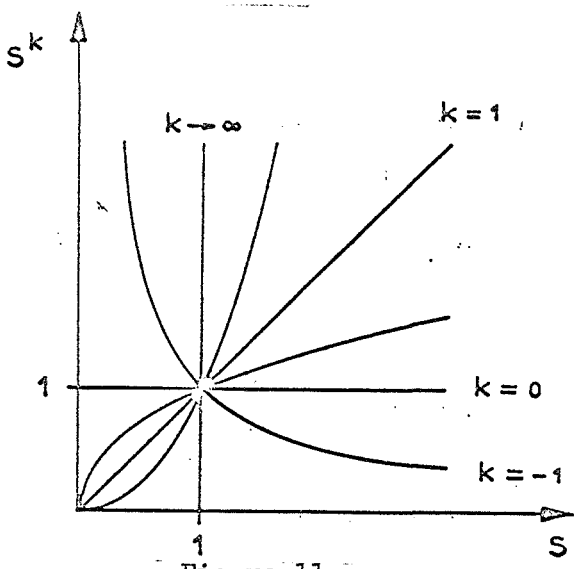

Figure 11.

where $C_z(x)$ is the value obtained for an (n x n) division. Placing $s = \frac{1}{m}$ and $t = \frac{1}{n}$,

$$C_z = C_z\left(\frac{1}{i}\right) + \int_i^0 \frac{dC_z}{ds}\, ds. \qquad (22)$$

From the three divisions which were made, it is possible to determine two points of the curve $\frac{dC_z}{ds}(s)$. Extension to s = 0 is easily made by means of the family of curves $\frac{dC_z}{ds} = a.s^k$ (Figure 11).

Application of this correction to the rectangular wing in torsion gives for $\beta A = 2$, M = 2, $\Omega = 1$:

$$100\ \delta C_z/|C_z| = 0{,}25 + i\ 0{,}15$$
$$100\ \delta C_{mx}/|C_{mx}| = -0{,}07 + i\ 0{,}10$$

instead of:

$$100\ \delta C_z/|C_z| = -0{,}37 + i\ 1{,}04$$
$$100\ \delta C_{mx}/|C_{mx}| = -0{,}6 + i\ 0{,}71.$$

IV.6. Study of a Delta Wing — Comparison with Other Methods

In the case of a non-rectangular wing, delta for example, the interaction of the upstream current sheets on the left and right has not allowed analytic calculation of the solution. Since the method presented here is very general, it is possible to carry out such calculations and to compare the results with those obtained by the method of M. Fenain and D. Guiraud-Vallée [9] and that of L. Darovsky and R. Dat (14], the latter being based on the solution of the integral equation which expresses the slopes as functions of the C_p.

The delta wing in the comparison was studied at M = $\sqrt{2}$ for a length $A = 2$, a reduced frequency $\Omega = 0.5$, first in bending, then in torsion.

For bending, the first calculation did not include the effects of curvature of the upstream current surface, i.e., of the coefficients A_j^i; Figure 12 shows the relatively large oscillations of the C_p curves in this case. A second

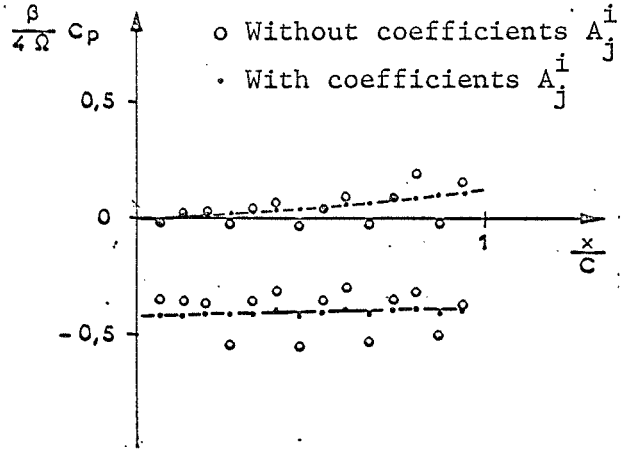

Figure 12.

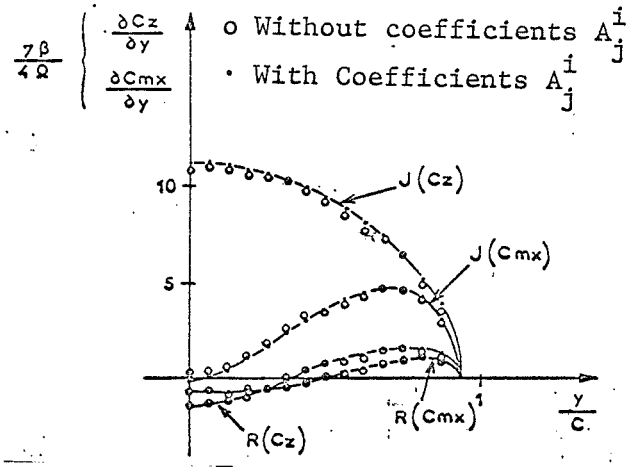

Figure 13.

calculation included the coefficients A_j^i, and the oscillations are about one-tenth as large. It is possible to draw the C_p curves with good accuracy.

After integration over x there is a poor definition of the distribution of C_z and C_{mx} at the T.E. in the first case, while the points "follow along" very well for the second calculation (Figure 13). Over all, the difference is only about 0.5% in the real part and 2% in the imaginary part, which leads one to hope that the weak residual oscillation would contribute only 0.1 to 0.2% in the final result. /12

The two numerical methods for comparison have about 5% [accuracy] in the opinion of the authors, and the results confirm these evaluations. However, the computations on the rectangular wing give hope of an accuracy of the order of 1%. This is why a comparison was made between:

(a) the errors which appear in the comparison methods for stable flow, relative to the analytical values; and

(b) the differences between those and the method proposed here.

The results are given in Table V.

It should be noted that the similarities are most striking in the imaginary part for bending and in the real part for torsion, which was predictable since, when $\Omega \to 0$, the imaginary part for bending, divided by Ω, approaches the plane

TABLE V.

Steady analytic value			Method of Fenain and Guiraud-Vallée		Method of Darovsky and Dat	
	C_z	C_{mx}	$100\,\frac{\delta C_z}{\lvert C_z\rvert}$	$100\,\frac{\delta C_{mx}}{\lvert C_{mx}\rvert}$	$100\,\frac{\delta C_z}{\lvert C_z\rvert}$	$100\,\frac{\delta C_{mx}}{\lvert C_{mx}\rvert}$
	2,594	0,4323	+ 4,1	+ 4	+ 1,4	— 5
Proposed unsteady method			Bending			
$\mathcal{R}$	0,04516	0,0073	+ 0,9	+ 0,6	+ 1,7	— 1,8
J	1,2112	0,1935	+ 4,5	+ 3,7	+ 0,9	— 5,4
			Torsion about the mid-chord			
$\mathcal{R}$	2,5595	0,4309	+ 4,8	+ 4,1	1,2	— 4
J	0,6141	0,265	+ 0,6	+ 3,1	0,7	— 3,2

plate lift effect for stationary flow, while in torsion it is the real part which approaches the same lift effect.

V. Conclusion

Inclusion of fundamental corrections has allowed an accuracy of the order of 1% in the treatment of wings in steady or unsteady flow, even for complicated shapes or modes.

Further, a study of convergence of the results as a function of the fineness of division was carried out systematically; the correction derived from it allows a further improvement in accuracy, and evaluation of the residual error. This increase in accuracy corresponds to no more than 1/10 the total computation time, while this [total] computer time would be multiplied by about ten for a finer division giving the same accuracy.

Indeed, the calculation of the coefficients K_j^i and A_j^i which allow reduction of the error from the order of 10% to 1% at constant division represents

only one quarter of the total computer time for a 20 x 20 division; for an N x N division, the time is proportional to N, while the calculation of the influence coefficients is proportional to N^2, and that of ϕ is, properly, to N^4.(3) Further, the computation of a series of modes, frequencies, and Mach numbers requires calculation of truncation and influence coefficients for a large number of cases. For example, on the Univac 1108 an isolated calculation in a 20 x 20 division takes two seconds, while each one in a series of calculations takes one second. If a greater accuracy were desired, a 40 x 40 division would require 15 seconds for each isolated calculation, and ten seconds for each one of a group. This 40 x 40 division is the presently acceptable limit for the program; an appreciable improvement in accuracy would lead to computing times greater than a minute, which does not seem useful since the accuracy of the calculations presented here has been obtained with only the 20 x 20 division.

Manuscript submitted 6 June 1969

---

(3) N^2 points of calculation, with computing time proportional to N^2 for each of them.

REFERENCES

1. Puckett, A.E. Supersonic wave drag of thin airfoils. J.A.S. (Sept. 1946), pp. 475-484.

2. Evvard. Use of source distributions for evaluating theoretical aerodynamics of thin finite wings at supersonic speed. NACA Report 951 (1950).

3. Hancock, G.J. Notes on thin wing theory at low supersonic speeds. The Aeronautical Quarterly, Part I (August 1959), Part II (November 1959).

4. Garrick, I.E., and S.I. Rubinow. Theoretical study of air forces on an oscillating or steady thin wing in a supersonic main stream. NACA T.R. 872 (1947).

5. Pines, S., and Alii. Application of aerodynamic flutter derivatives to a flexible wing with supersonic and subsonic edges. Republic Aviation Corporation Report E. SAF 2 (1954). /13

6. Li, Ta. Aerodynamic influence coefficients for an oscillating finite thin wing in supersonic flow. J.A.S., Vol. 23 (1956).

7. Zartarian, G., and Alii. Application of numerical integration techniques to the low-aspect-ratio flutter problem in subsonic and supersonic flow. M.I.T. Report 52-3 (1954).

8. Stark, J.E.V. Calculation of aerodynamic forces on two oscillating finite wings at low supersonic Mach numbers. Saab T.N. 53.

9. Fenain, M., and D. Guiraud-Vallée. Numerical calculation of wings in supersonic flow. Rech. Aer., Part 1, No. 115 (1966), Part 2, No. 116 (1967).

10. Brun-Gabriel, J.M. Principle and study of the conditions for use of an electric calculator for wings in linearized supersonic flow. Third Thesis, Paris (January 1963).

11. Germain, P. General theory of conical movements and its applications to supersonic aerodynamics. ONERA Publication No. 34 (1949).

12. Miles, J.W. The oscillating rectangular airfoil at supersonic speeds. Quart. Appl. Math., Vol. 9 (1951), pp. 47-65.

13. De Jager, E.M. Oscillating rectangular wings in supersonic flow with arbitrary bending and torsion mode shapes. N.L.R. Report W3 Nat. Aeronaut. Research Inst., Amsterdam (1959).

14. Darovsky, L., and R. Dat. Determination of unsteady aerodynamic forces. AGARD Report 512 (1965).

SUMMARY BIBLIOGRAPHY

1. Princeton University. High Speed Aerodynamics and Jet Propulsion. Vol. VI and VII. General bibliography up to 1957.

2. Germain, P. Some recent progress in theoretical high-speed aerodynamics. Transactions of the IXth International Congress on Applied Mechanics. Vol. I (1957). Reference bibliography.

3. James, R.M. Comments and numerical experiments concerning the computation of steady and unsteady linear thin wing theory. McDonnel-Douglas Report DAC 66 765 (January 1968).

4. Woodward, F.A., and J.W. Larsen. A method of optimising camber surfaces for wing-body combinations at supersonic speeds. Boeing Document D6-10741 (1965).

5. Enselme, M. Contribution of electrical analogs to the calculation of the aerodynamic characteristics of an air-ship in stable or unstable supersonic flow. ONERA Publication No. 119 (1967).

Translated for National Aeronautics and Space Administration under contract No. NASw 2035, by SCITRAN, P. O. Box 5456, Santa Barbara, California, 93103.